Tunable liquid crystal q-plates with arbitrary topological charge

Sergei Slussarenko,[1,*] **Anatoli Murauski,**[2] **Tao Du,**[2]
Vladimir Chigrinov,[2] **Lorenzo Marrucci,**[1,3] **and Enrico Santamato**[1]

[1]*Dipartimento di Scienze Fisiche, Università di Napoli "Federico II", Complesso Universitario di Monte S. Angelo, 80126 Napoli, Italy*
[2]*Hong Kong University of Science and Technology, Clear Water Bay, Kowloon, Hong Kong*
[3]*CNR-SPIN, Complesso Universitario di Monte S. Angelo, I-80126 Napoli, Italy*

[*]*sergei.slussarenko@na.infn.it*

Abstract: Using a photoalignment technique with a sulphonic azo-dye as the surfactant aligning material, we fabricated electrically tunable liquid crystal q-plates with topological charge 0.5, 1.5 and 3 for generating optical vortex beams with definite orbital angular momentum (OAM) 1,3 and 6 per photon (in units of $\hbar$), respectively. We carried out several tests on our q-plates, including OAM tomography, finding excellent performances. These devices can have useful applications in general and quantum optics.

© 2011 Optical Society of America

OCIS codes: (160.3710) Liquid crystals; (050.4865) Optical vortices.

References and links

1. L. Allen, M. W. Beijersbergen, R. J. C. Spreeuw, and J. P. Woerdman, "Orbital angular momentum of light and the transformation of Laguerre-Gaussian laser modes," Phys. Rev. A **45**, 8185–8189 (1992).
2. S. Franke-Arnold, L. Allen, and M. J. Padgett, "Advances in optical angular momentum," Laser Photon. Rev. **2**, 299–313 (2008).
3. A. Jesacher, S. Fürhapter, S. Bernet, and M. Ritsch-Marte, "Shadow effects in spiral phase contrast microscopy," Phys. Rev. Lett. **94**, 233902 (2005).
4. G. Gibson, J. Courtial, M. J. Padgett, M. Vasnetsov, V. Pasko, S. M. Barnett, and S. Franke-Arnold, "Free-space information transfer using light beams carrying orbital angular momentum," Opt. Express **12**, 5448–5456 (2004).
5. A. Mair, A. Vaziri, G. Welhs, and A. Zeilinger, "Entanglement of the angular momentum states of photons," Nature **412**, 313–315 (2001).
6. J. T. Barreiro, N. K. Langford, N. A. Peters, and P. G. Kwiat, "Generation of hyperentangled photon pairs," Phys. Rev. Lett. **95**, 260501 (2005).
7. G. Molina-Terriza, J. P. Torres, and L. Torner, "Twisted photons," Nat. Phys. **3**, 305–310 (2007).
8. L. Aolita and S. P. Walborn, "Quantum communication without alignment using multiple-qubit single-photon states," Phys. Rev. Lett. **98**, 100501 (2007).
9. M. W. Beijersbergen, R. P. C. Coerwinkel, M. Kristensen, and J. P. Woerdman, "Helical-wavefront laser beams produced with a spiral phaseplate," Opt. Commun. **112**, 321–327 (1994).
10. M. W. Beijersbergen, L. Allen, H. van der Veen, and J. P. Woerdman, "Astigmatic laser mode converters and transfer of orbital angular momentum," Opt. Commun. **96**, 123–132 (1993).
11. V. Y. Bazheov, M. S. Soskin, and M. V. Vasnetsov, "Screw dislocations in light wavefronts," J. Mod. Opt. **39**, 985–990 (1992).
12. Y. Igasaki, F. Li, N. Yoshida, H. Toyoda, T. Inoue, N. Mukohzaka, Y. Kobayashi, and T. Hara, "High efficiency electrically-addressable phase-only spatial light modulator," Opt. Rev. **6**, 339–344 (1999).
13. L. Marrucci, C. Manzo, and D. Paparo, "Optical spin-to-orbital angular momentum conversion in inhomogeneous anisotropic media," Phys. Rev. Lett. **96**, 163905 (2006).
14. L. Marrucci, C. Manzo, and D. Paparo, "Pancharatnam-Berry phase optical elements for wavefront shaping in the visible domain: switchable helical modes generation," Appl. Phys. Lett. **88**, 221102 (2006).
15. E. Karimi, B. Piccirillo, E. Nagali, L. Marrucci, and E. Santamato, "Efficient generation and sorting of orbital angular momentum eigenmodes of light by thermally tuned q-plates," Appl. Phys. Lett. **94**, 231124 (2009).

16. B. Piccirillo, V. DAmbrosio, S. Slussarenko, L. Marrucci, and E. Santamato, "Photon spin-to-orbital angular momentum conversion via an electrically tunable q-plate," Appl. Phys. Lett. arXiv:1010.4473 (in press).
17. E. Karimi, S. Slussarenko, B. Piccirillo, L. Marrucci, and E. Santamato, "Polarization-controlled evolution of light transverse modes and associated pancharatnam geometric phase in orbital angular momentum," Phys. Rev. A **81**, 053813 (2010).
18. E. Nagali, L. Sansoni, F. Sciarrino, F. De Martini, L. Marrucci, B. Piccirillo, E. Karimi, and E. Santamato, "Optimal quantum cloning of orbital angular momentum photon qubits through hong-ou-mandel coalescence," Nat. Photon. **3**, 720–723 (2009).
19. S. Nersisyan, N. Tabiryan, D. M. Steeves, and B. R. Kimball, "Fabrication of liquid crystal polymer axial wave-plates for uv-ir wavelengths," Opt. Express **17**, 11926–11934 (2009).
20. P. G. de Gennes, *The Physics of Liquid Crystals* (Oxford University Press, Oxford, 1974).
21. The strong anchoring at both the sample walls prevents the decay of the otherwise unstable disclination lines with integer q.
22. V. G. Chigrinov, V. M. Kozenkov, and H.-S. Kwok, *Photoalignment of Liquid Crystalline Materials: Physics and Applications* (Wiley Publishing, 2008).
23. D. F. V. James, P. G. Kwiat, W. J. Munro, and A. G. White, "Measurement of qubits," Phys. Rev. A **64**, 052312 (2001).
24. The fidelity of the measured state $|\psi\rangle$ with respect to the expected state $|\psi_0\rangle$ is usually defined as $\langle\psi|\psi_0\rangle^2$.
25. B. Jack, J. Leach, H. Ritsch, S. M. Barnett, M. J. Padgett, and S. Franke-Arnold, "Precise quantum tomography of photon pairs with entangled orbital angular momentum," N. J. Phys. **11**, 103024 (2009).
26. E. Nagali, F. Sciarrino, F. De Martini, L. Marrucci, B. Piccirillo, E. Karimi, and E. Santamato, "Quantum information transfer from spin to orbital angular momentum of photons," Phys. Rev. Lett. **103**, 013601 (2009).

1. Introduction

A light beam has two "rotational" degrees of freedom: spin angular momentum (SAM) and orbital angular momentum (OAM). The first is associated to the polarization of the transverse electric field and may take the values $s = \pm\hbar$ per photon, that correspond to circular left and right polarization, respectively. OAM is associated to the phase structure of the complex electric field and paraxial beams with a helical phase front defined by the factor of $\exp(i\ell\varphi)$ carry a definite amount of OAM per photon equal to $\ell\hbar$, where ℓ can take any integer value [1, 2]. In last years, beams carrying OAM have received an increased attention in classical [3, 4] and quantum optics [5–8]. Till now, few methods of OAM-carrying beam generation were proposed, namely spiral phase plates [9], astigmatic lens converters [1, 10] and computer generated fork holograms (CGH) [11] in conjunction with spatial light modulators (SLMs) [5, 12]. All these methods have in terms of efficiency, working speed and stability or have specific requirements for the input light state.

Recently, a novel device based on liquid crystal (LC) technology, able to generate and manipulate the OAM was introduced [13, 14]. This device, called "q-plate" (QP) is essentially a birefringent wave plate with inhomogeneous patterned distribution of the local optical axis in the transverse plane. The pattern of the optical axis distribution is defined by a semi-integer topological charge "q". When a circularly polarized light beam traverses the QP, a $\pm 2q$ amount of OAM (in units of $\hbar$) is transferred into the beam, with the sign determined by the input polarization helicity. The efficiency of this conversion is given by the optical retardation δ of the QP, that can be controlled by temperature [15] or electrical field, as made in this work [16]. QPs can be very efficient, fast and stable, although they are less flexible than SLMs as they address only a OAM two-dimensional subspace.

Till now, only $q = 1$ QPs were realized with LCs. Such device has already found a number of applications in various fields of optics [17, 18]. Polymer based QPs were manufactured elsewhere [19], but such QPs, being solid and non-tunable, are suitable for single wavelength, require accurate control of thickness during manufacturing and cannot be used in applications where the conversion efficiency must be changed or switched. In this paper we report the realization of LC-based δ-tunable QPs with arbitrary topological charge by a photoalignment technology and demonstrate examples of QPs with $q = 0.5, 1.5$ and 3.

2. Q-plate structure and fabrication

In the QP, the LC film is enclosed between glass walls perpendicular to the z-axis. The orientation of the local optical axis of the QP is given by the LC molecular director distribution $\boldsymbol{n(r)} = (\sin\theta\cos\alpha, \sin\theta\sin\alpha, \cos\theta)$, with $\theta = \theta(\boldsymbol{r}), \alpha = \alpha(\boldsymbol{r})$ being the polar angles. The walls of the QPs are coated for parallel strong anchoring ($\theta = \pi/2$) and the the surface alignment profile is made so to have $\alpha(x,y) = \alpha(\varphi) = q\varphi + \alpha_0$ in the LC bulk, where $\varphi = \arctan(y/x)$ is the transverse azimuthal coordinate, α_0 is a real number, and q is an integer or half integer number. The surface texture induced by this distribution is known in the physics of LC as a Schlieren structure with an isolated point defect (or "noyau") of topological charge q at the wall center [20]. The "noyaux" in the two walls of the cell are carefully aligned along the z axis during the cell manufacturing, so that a disclination line of same charge q is generated in the bulk (from here the name q-plate of the device). As it is well known from the elastic theory of LC, the equivalence between $\boldsymbol{n}$ and $-\boldsymbol{n}$ implies that the charge q is either integer or half-integer [21].
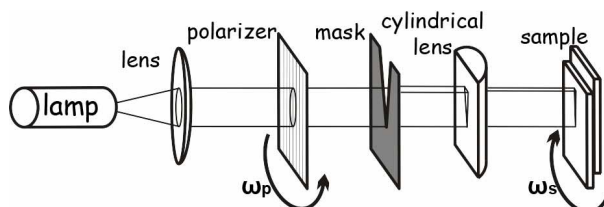
Fig. 1. (Color online) QP fabrication setup scheme.

The traditional way to manufacture a cell with planar alignment of liquid crystal is to rub the inner sides of the glass walls, previously coated with thin layer of polyimide, with velvet fabric. The rubbing direction defines the anisotropy of the surface that, in turn, orient the LC molecules perpendicular (or parallel, depending on the LC type) to the rubbing direction. The $q = 1$ QPs can be manufactured in this way, by rubbing the cell walls with a rotating piece of fabric [13, 15]. Other patterns, with $q \neq 1$ cannot be made by this method. In this work, we employed a photoalignment technique. The scheme of our setup is shown in Fig. 1. The LC cell was made from two glass substrates, spin-coated with 1% solution of sulphonic azo-dye SD1 (Dainippon Ink and Chemicals) in dimethylformamide (DMF) for 30 s at 3000 rpm. The glass windows were coated with conducting Indium-Tin-Oxide (ITO) to apply and external electrical field to the LC film. After the evaporation of the solvent, by soft-baking at 120 °C for 5 min, the glasses were assembled together and 6 μm dielectric spacers were used to define the cell gap. A mercury lamp of 180 mW/cm^2 power density was used as the collimated light source. The light beam was polarized by a linear wiregrid polarizer and made to pass through an angular mask of 10° angular aperture. After the mask, a cylindrical lens was used to focus and converge the selected sector on the cell. The SD1 surfactant provides planar alignment for the LC in the direction perpendicular to the writing light polarization, with anchoring energy comparable with the polyimide rubbing based alignment [22]. Both polarizer and sample were attached to rotating mounts controlled by PC through step-motors. The rotation step of the sample was set to 2°. An exposure time of 2 hours and one complete turn of the sample was enough to provide high quality alignment of the LC film in all our QPs. Such values, together with the angular aperture of the mask, resulted from a compromise between having enough light passing through the mask and having a small enough image of the mask on the cell to obtain an acceptable smoothly varying local surface alignment. To make QPs with very large

q value smaller mask angular aperture would be necessary. By adjusting the ratio between the angular speeds of the two motors, different topological charges were impressed on the cell walls. It can be easily shown that the induced topological charge is given by $q = 1 \pm \frac{\omega_p}{\omega_s}$, where ω_p and ω_s are the angular speeds of the polarizer and sample, respectively, and the "+" and "−" signs correspond to opposite and same rotation direction of the two mounts, respectively. After the exposure, the samples were filled with the LC (MLC 6080 mixture from Merck) and sealed by epoxy glue. Heating the sample above the LC clearing point and subsequent slow cooling helped to remove occasional LC alignment defects. Topological charges $q = 0.5, 1.5, 3$, as shown in Fig. 2(a-c), were realized with the procedure described above. However any semi-integer charge can be realized, in principle, with this technique.
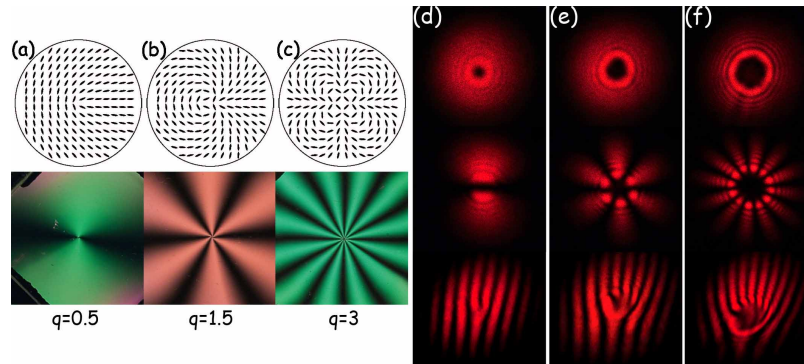

Fig. 2. (Color online) (a-c) Examples of the LC patterns with different topological charges and photos of the corresponding samples under crossed polarizers. (d-f) CCD pictures of the intensity beam profiles generated by the QPs shown in (a-c) when they are tuned. The input beam polarization was circularly polarized (top) or linearly polarized (middle). The respective interference patterns with a plane wave are also shown (bottom).

3. Optical characterization

When a beam traverses a QP with topological charge q and phase retardation δ, a fraction $\sin^2 \frac{\delta}{2}$ of the photons in the beam have their SAM reversed and change their OAM by an amount $\pm 2q$. More precisely, the photons flipping their spin from -1 to $+1$ (-1 to $+1$) change their OAM of $-2q$ ($+2q$). The remaining photon fraction $\cos^2 \frac{\delta}{2}$ remain in their initial SAM and OAM state. [13, 14] When the phase retardation of the QP is tuned to half-wave ($\delta = \pi$) all the input photons will be converted. In the particular case of charge $q = 1$, the total SAM+OAM light angular momentum remains unchanged in passing through the QP, so that the change of the photon SAM is transferred into a corresponding opposite change of the photon OAM, yielding a spin-to-OAM conversion (STOC) [13]. For a single photon, a similar action takes place on two wave-function components, with amplitudes $\sin \frac{\delta}{2}$ and $\cos \frac{\delta}{2}$ respectively.

The preliminary test on our QPs was just to observe the intensity pattern generated by the QP for a circularly or linearly polarized TEM_{00} incident beam. The observed intensity patterns are shown in Fig. 2(d-f, top and middle row). In the case of the circular polarization of the incident beam the we found the typical doughnut profile of vortex beam, while for the linear input polarization the intensity pattern shows a number $4q$ of bright radial lobes, as foreseen from theory. To better demonstrate the capability of our QPs to generate optical vortices a measurement of the helical phase front is desirable. Such measurement was done by inserting the QP into one arm of a Mach-Zehnder interferometer and by registering the interference pattern with a reference wave. The interference patterns, in the case of a plane reference wave

at small angle, have a typical "fork"-like structure [11], in which interference fringes have a disclination, where the optical vortex is located. The disclination order (i.e. the splitting of the interference line into a higher number of lines) corresponds to the OAM value of the beam, as shown in Fig. 2(d-f, bottom row). We tested also the STOC efficiency of our QPs, defined as the ratio between the STOC converted power and the total power in the output. This measurement was done by registering the power fraction of the light transmitted by the QP having polarization orthogonal to that of the incident beam. The QP conversion efficiency was changed by changing the QP retardation δ by applying an external voltage. To avoid electro-chemical effects, we applied a 2 kHz square-shaped voltage. The measurements were done at 543.5 nm and 633 nm light wavelengths. The results for the $q = 0.5$ QP are shown in Fig. 3(a). We obtained a STOC efficiency of up to 99% for all fabricated QPs. Due to unavoidable reflection, diffusion, and absorption losses in the QP, the overall STOC efficiency defined as the ratio between the STOC converted power in the output and the total incident power was found about 86% for all our QPs. These losses, however, could be easily avoided by adding an antireflection coating.
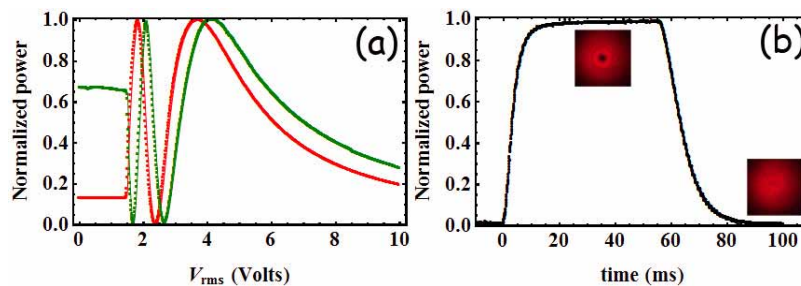

Fig. 3. (Color online) (a) – fraction of the output power converted by STOC in the QP as a function of the applied voltage. Red line - 633 nm input beam wavelength, green line - 534.5 nm input beam wavelength. (b) – time behavior of the QP upon sending two consecutive AC pulses that correspond to the minimum and maximum conversion efficiency. The intensity patterns in the insets show the on-off switching of the vortex beam with $\ell = 1$. The data refer to the QP with $q = 0.5$.

Since the STOC efficiency measurement was based on the polarization state of the beam only, an additional detailed study of the beam phase structure is required. For doing this we measured directly the OAM content of the beam generated by the QP, tuned to the maximum conversion, exploiting a tomographic technique [23]. Since we were not interested in the beam polarization, we fixed it by inserting a linear polarizer after the QP and carried out only the tomography of the beam OAM content. The main advantage of the optical tomography is that both amplitude and phase of the OAM components of a light beam can be reconstructed and that also the "fidelity" of the beam OAM state with respect to a given theoretical state can be evaluated [24]. Because the tomographic characterization is a very long procedure, we performed this test on the $q = 0.5$ QP only, restricting the OAM states to the Hilbert space spanned by the opposite OAM eigenvalues $\ell = \pm 1$. In the experiment, the $q = 0.5$ QP was used to generate the states $|1\rangle_o, |-1\rangle_o$, and $1/\sqrt{2}(|1\rangle_o - |-1\rangle_o)$, as described above, and a set of six computer-generated holograms (CGH) was sent into a spatial light modulator (SLM) to project the given beam state into the corresponding OAM bases [25, 26]. The density matrices of the measured states are reported in Fig. 4(a)-(c). The measurements showed an average fidelity of $98 \pm 1\%$ of the generated states with the expected ones. We tested also the correlation between the circularly right polarized fraction of the beam coming from the $q = 0.5$ QP and the power of the $\ell = 1$ component of the same beam for different elliptically polarized states of the input TEM_{00} beam. The measurements were carried on with a circular polarizer to select the right handed
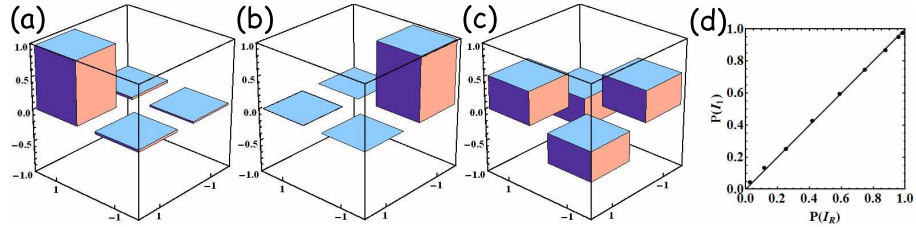
Fig. 4. (Color online) (a)-(c) – the real components of the density matrices of the OAM states, reconstructed via quantum tomography process for the $|1\rangle_o, |-1\rangle_o$ and $\frac{1}{\sqrt{2}}(|1\rangle_o - |-1\rangle_o)$ states respectively. (d) - fraction of the $\ell = 1$ beam intensity as the function of the fraction of the right polarized output beam, for different elliptically polarized inputs. The data refer to the QP with $q = 0.5$

polarization and a suitable fork hologram to select the $\ell = 1$ OAM component. The results are shown in Fig. 4(d). We found a standard deviation of $\sigma = 0.02$ from perfect one-to-one correlation between the circular right polarization state of photons and their OAM value $\ell = 1$. As the final test, we measured the switching speed of the QP with $q = 0.5$ between the last minimum conversion point where the output beam has $\ell = 0$ and the last maximum conversion point where the output beam has $\ell = 1$. These points are located at 2.4 and 3.7 Volts rms in Fig. 3, respectively (for 633 nm). The switching times were found to be around 25-30 ms, as shown in Fig. 3(b). The intensity profiles in the insets show the on-off switching of the vortex beam with $\ell = 1$.

4. Conclusions

In conclusion, using a photoalignment technique we realized several nematic liquid crystal QPs with the topological charge q different from $q = 1$, including fractionary half-integer charges. The optical phase retardation of our QPs can be tuned by external electric field, that allows to simplify the manufacturing procedure, removing particular requirements for the cell gap and reach high conversion efficiencies (up to 99%) for different wavelengths of the input light in real time. Our method is siutable for manufacturing tunable q-plates with arbitrary charge q.

Acknowledgments